Can a nightside geomagnetic Delta H observed at the equator manifest a penetration electric field?

Y. Wei,[1] M. Fraenz,[1] E. Dubinin,[1] M. He,[2] Z. Ren,[3] B. Zhao,[3] J. Liu,[3] W. Wan,[3] K. Yumoto,[4] S. Watari,[5] and S. Alex[6]

Received 22 July 2012; revised 4 February 2013; accepted 5 February 2013; published 6 June 2013.

[1] A prompt penetration electric field (PPEF) usually manifests itself in the form of an equatorial ionospheric electric field being in correlation with a solar wind electric field. Due to the strong Cowling conductivity, a PPEF on the dayside can be inferred from Delta H (ΔH), which is the difference in the magnitudes of the horizontal (H) component between a magnetometer at the magnetic equator and one off the equator. This paper aims to investigate the performance of ΔH in response to a PPEF on the nightside, where the Cowling conductivity is not significant. We first examine the strongest geomagnetically active time during the 20 November 2003 superstorm when the Dst drops to −473 nT and show that the nightside ΔH can indeed manifest a PPEF but with local time dependence and longitude dependence. We then examine a moderately active time by taking advantage of the multiple-penetration event during 11–16 November 2003 when the Dst remains greater than −60 nT. During this event, a series of PPEF pulses recorded in Peru, Japan, and India form a database, allowing us to examine PPEF effects at different local times and longitudes. The results show that (1) the nightside ΔH was caused by attenuation of the effects of the polar electric field with decreasing latitude; (2) the nightside ΔH can manifest a PPEF at least in the midnight-dawn sector (0000–0500 LT), but not always; and (3) the magnitude of the nightside ΔH in the midnight-dawn sector in Peru is on average only 1/18 of that of the dayside ΔH in response to a given PPEF.

Citation: Wei, Y., et al. (2013), Can a nightside geomagnetic Delta H observed at the equator manifest a penetration electric field?, *J. Geophys. Res. Space Physics*, *118*, 3557–3567, doi:10.1002/jgra.50174.

1. Introduction

[2] The correlations between a low-latitude ionospheric electric field and the interplanetary magnetic field (IMF) or interplanetary electric field (IEF) are often observed during geomagnetic disturbances, and these are usually termed "electric field penetrations" or "prompt electric field penetrations" [*Kelley*, 1989; *Fejer*, 2002]. *Nishida* [1968] was the first to notice that geomagnetic fluctuations are coherent with the IMF variations in its north-south component, and *Rastogi* [1977] found that the equatorial geomagnetic field can respond to a reversal of the IMF from southward to northward. These pioneer studies pointed out that a prompt penetration electric field (PPEF) drives geomagnetic disturbance. With more comprehensive data sets, *Kikuchi et al.* [1996] described a fairly complete picture of geomagnetic responses to the PPEF. However, magnetometers can only tell the strength of the two-dimensional (2-D) equivalent ionospheric current, and one needs to assume a conductance to infer the driving electric field to study the PPEF. The incoherent scatter radar (ISR) at Jicamarca (JIC) is a more powerful instrument for measuring electric fields that measures the plasma vertical drift, and its database has been used to quantitatively determine the relationship between the IEF and the PPEF [e.g., *Fejer and Scherliess*, 1997; *Kelley et al.*, 2003]. But a limitation of the ISR data set is its lack of continuous observation; in other words, the data set is too sporadic to fully meet the requirements of PPEF-related studies.

[3] A new data set has been emerging in recent decades as a solution to combine the advantages of magnetometer and ISR data. *Anderson et al.* [2002] suggested a linear relationship between ISR vertical drift and Delta H (ΔH) in Peru. Here the ΔH is the difference in the magnitudes of the horizontal (H) component between a magnetometer placed directly on the magnetic equator (JIC, dip 0.8°N) and one displaced 6° to 9° away [Piura (PIU), dip 6.8°N]. At a given

[1]Max Planck Institute for Solar System Research, Katlenburg-Lindau, Germany.
[2]Campus Ring 1, Jacobs University Bremen, Bremen, Germany.
[3]Beijing National Observatory of Space Environment Institute of Geology and Geophysics, Chinese Academy of Sciences, Beijing, China.
[4]Department of Earth and Planetary Sciences, Kyushu University, Fukuoka, Japan.
[5]National Institute of Information and Communications Technology, Tokyo, Japan.
[6]Indian Institute of Geomagnetism, New Panvel (W), Navi Mumbai, India.

Corresponding author: Y. Wei, Max Planck Institute for Solar System Research, Max-Planck-Str. 2, DE-37191 Katlenburg-Lindau, Germany. (wei@mps.mpg.de)

2169-9380/13/10.1002/jgra.50174

point on the dayside equator, the logic chain from the ΔH to the vertical drift is quite clear: the ΔH is linearly related to the strength of the equatorial electrojet (EEJ), the EEJ is linearly related to the electric field, and the electric field is linearly associated with the vertical drift ($\mathbf{V} = \mathbf{E} \times \mathbf{B}/B^2$). Although this logic chain does not exist on the nightside due to the absence of significant Cowling conductivity, calculation of the ΔH has become a popular method to identify a PPEF with the ΔH having been measured by JIC and PIU in Peru [e.g., *Huang et al*., 2005; *Wei et al*., 2010, 2011], Yap (YAP, dip 1.6°N) and Okinawa (OKI, dip 19.5°N) in Japan [e.g., *Fejer et al*., 2007; *Kikuchi et al*., 2010], as well as Tirunelveli (TIR, dip 0.5°S) and Alibag (ABG, dip 10°N) in India [e.g., *Kelley et al*., 2007; *Veenadhari et al*., 2010]. The locations of these three pairs of stations are shown in Figure 1. The daily electric field database inferred from the JIC-PIU ΔH is currently available at the Jicamarca Radio Observatory (http://jro.igp.gob.pe/).

[4] Recent papers related to the PPEF have shown a rising interest in simultaneous measurements of ΔH at different longitudes [e.g., *Kelley et al*., 2007]. The PPEF is known to be of global scale and has strong local time dependence in its penetration efficiency as shown by early simulation work [e.g., *Nopper and Carovillano*, 1978]. However, because there is only one ISR located at the equator, one has to seek other data sets to conduct observational studies at multiple longitudes. For example, *Kelley et al*. [2007] compared the Peru vertical drift measured by the ISR with the India vertical drift inferred from the time derivative of the F-layer height as measured by an ionosonde and concluded that "the magnitudes of the daytime and nighttime penetration electric fields are comparable and hence are of global large scale." On the other hand, more studies have utilized ΔH data sets, mainly because geomagnetic observations are more continuous. We noted that several recent papers reported discernible PPEF signatures in the ΔH on the nightside, where the Cowling conductivity is very weak. For example, during the November 2004 superstorm, the YAP-OKI ΔH at 0400–0600 LT was found to exhibit exceptionally large westward current perturbations when the JIC ISR simultaneously observed a very strong PPEF at 1400–1600 LT (see figure 4 of *Fejer et al*. [2007]). The authors treated both as PPEF effects but did not give further explanations. For another example, during an intense storm, the dayside ΔH in Peru and the nightside ΔH in Japan were found to be related to the PPEF (see figure 1 of *Galav et al*. [2011]). Since the nightside ΔH must have a different origin from the dayside ΔH due to the lack of significant Cowling conductivity on the nightside ionosphere, naturally, such questions as "Can nightside ΔH be an indicator of the PPEF?" and "What is the local time range from which we can use ΔH to identify the PPEF?" arise.

[5] The motivation of this paper is to find some clues. We will first examine the strongest geomagnetically active time during the 20 November 2003 superstorm when the Dst drops to −473 nT. The extremely large PPEF during some superstorms may have significant effects on the nightside ΔH, because superstorms "drive the magnetosphere to an extreme state where dynamic processes, obscure under lesser conditions, can be clearly identified and studied" [*Bell et al*., 1997]. We then examine a moderately active time by taking advantage of the multiple-penetration event during 11–16 November 2003 when the Dst remains greater than −60 nT. This event was first reported by *Wei et al*. [2008a], who found that the IEF associated with fluctuations of the IMF B_Z in the south-north direction impulsively penetrated the equatorial ionosphere without shielding. The characteristics of solar wind during this event have been presented in detail by *Tsurutani et al*. [2010], and the relationship between the IEF and the vertical drift measured by ISR has also been described very well by *Kelley and Dao* [2009]. We thus will not repeat these studies and instead directly focus on the vertical drift and ΔH.

[6] To our knowledge, the database obtained during this multiple-penetration event is unique for studying the above-cited two questions for several reasons: (1) The PPEF exhibits a multi-pulse-like pattern and persists for several days, and its source has been found to be mostly associated with the oscillating IMF [*Wei et al*., 2008a]. The disturbances of the equatorial electric field can also be produced by other external factors (such as changes in solar wind dynamic pressure [*Huang et al*., 2008; *Wei et al*., 2008b]) or be associated with other internal processes inside the magnetosphere (e.g., substorms [*Wei et al*., 2009]) or the ionosphere (e.g., disturbance dynamoelectric field [*Blanc and Richmond*, 1980]). However, none of them can generate a long-lasting, IMF-related, and multi-pulse-like pattern, and their contributions to electric field disturbance can be ignored for this multiple-penetration event. Therefore, if the multi-pulse-like disturbances appear in the nightside ΔH and are consistent with the global PPEF, then we could evaluate the performance of the nightside ΔH in response to the PPEF. (2) The ISR was continuously operating for 125 h, which is one of the longest intervals in the whole ISR database. This allows us to define a "standard PPEF" as a reference to evaluate the performance of the nightside

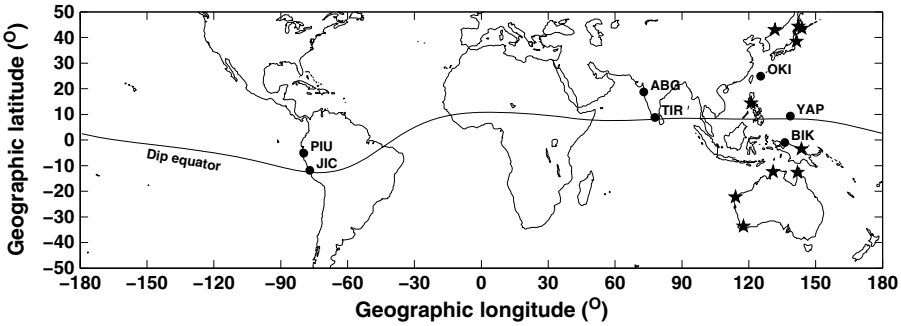

Figure 1. Locations of the geomagnetic stations listed in Table 1.

ΔH, because ISR measures electric fields for both the dayside and the nightside. The oscillating IEF or IMF cannot be used as a reference, because a duskward IEF pulse (associated with a southward IMF) probably causes a PPEF at the equator, but a dawnward IEF pulse generally does not. (3) The continuous ΔH data from Peru, India, and Japan provide a multi-longitude ΔH data set that simultaneously covers the dayside and the nightside. (4) There is no significant shielding electric field [*Wei et al*., 2008a], and this can avoid uncertainties introduced by variable shielding electric fields. Therefore, we can directly extract a PPEF from the ISR and ΔH data sets without considering shielding effects.

2. Data Sets and Observations

2.1. Data Sets

[7] The cross-polar cap potential (CPCP) will be used to illustrate the influence of the solar wind-magnetosphere interaction on the polar cap ionosphere. The CPCP is calculated by the assimilative Mapping of ionospheric electrodynamics (AMIE) procedure, which is a technique used to reconstruct high-latitude ionospheric electrodynamic parameters by combining various data sets [*Richmond and Kamide*, 1988; *Ridley et al*., 1998]. The CPCP is a proxy of plasma convection and associated convection electric fields; thus, it may represent the source of a PPEF. Some case studies have confirmed the relationship between AMIE-derived CPCP and the PPEF [e.g., *Wei et al*., 2010, 2011]. Furthermore, using the CPCP instead of the IEF can effectively avoid uncertainties in estimation of the time delay of solar wind propagating from the L1 point to the dayside magnetopause. This time delay was found to vary from day to day during 11–16 November 2003 [*Kelley and Dao*, 2009].

[8] We calculated ΔH at three pairs of equatorial stations (Figure 1) that have been frequently used to study the PPEF: JIC-PIU in Peru (LT = UT − 5), TIR-ABG (LT = UT + 5) in India, and YAP-BIK in Japan (LT = UT + 8.7). The ΔH can be calculated by two steps: (1) subtracting the H component at one station from the H component at another and (2) subtracting the mean value of the nightside interval (some studies take early morning minimum values). One may also take the second step first, because the PPEF is linearly related to the intensity of variations of ΔH rather than the absolute intensity thereof. As mentioned in section 1, it has been found that the nightside ΔH in Japan somehow responded to the PPEF; thus, we will use a middle- to low-latitude station chain (subject to mm210) in the Japan longitude sector to reveal the latitude profile of the H component. Especially, we will also calculate the YAP-OKI ΔH to examine the effect of the distance between two stations in evaluating the PPEF, because OKI is farther from YAP than BIK. The detailed locations of these stations are listed in Table 1.

Table 1. Locations of the Geomagnetic Stations

Station Name	Abbreviation	Geographic Coordinates (°)		Geomagnetic Coordinates (°)	
		Latitude	Longitude	Latitude	Longitude
Moshiri	MSR	44.4	142.3	37.6	213.2
Rikubetsu	RIK	43.5	143.8	34.7	210.8
Popov Island	PPI	42.9	131.7	36.6	203.6
Onagawa	ONW	38.4	141.5	31.7	212.5
Muntinlupa	MUT	14.4	121.0	3.6	191.6
Biak	BIK	−1.1	136.1	−12.2	207.3
Wewak	WWK	−3.6	143.6	−14.1	215.3
Darwin	DRW	−12.4	130.9	−23.1	202.7
Weipa	WEP	−12.7	141.9	−23.0	214.3
Learmonth	LEM	−22.2	114.1	−34.2	185.0
Katanning	KAT	−33.7	117.6	−46.6	188.2
Okinawa	OKI	24.8	125.3	14.5	195.7
Yap	YAP	9.3	138.5	−0.3	209.0
Tirunelveli	TIR	8.7	77.8	0.2	149.3
Alibag	ABG	18.6	72.9	9.5	143.3
Piura	PIU	−5.2	259.6	3.6	331.8
Jicamarca	JIC	−11.9	256.9	−3.9	329.8

2.2. Performance of the Nightside ΔH in Response to the PPEF During the 20 November 2003 Superstorm

[9] We first examine the performance of the nightside ΔH in response to the PPEF during superstorms. *Fejer et al*. [2007] already reported that the ΔH in Japan at 0400–0600 LT showed exceptionally large westward current perturbations when the JIC ISR simultaneously observed a very strong PPEF at 1400–1600 LT during the November 2004 superstorm. Note that this PPEF was controlled by the IEF. Here we study the most severe superstorm of solar cycle 23 during 20 November 2003, featuring the lowest Dst (−472 nT) in this solar cycle. The PPEF during this superstorm is controlled by solar wind density instead of the IEF when the CPCP is saturated [*Wei et al*., 2012]. A more important reason to choose this superstorm is that there is no significant shielding electric field, because the PPEF decoupled from the convection electric field in the magnetotail, and thus the shielding electric field in the ring current was not able to comply with the variations of the PPEF [*Wei et al*., 2012]. Therefore, this superstorm event allows us to examine the PPEF effect on the ΔH without considering the shielding electric field. Further details of this superstorm, especially the responses of the ionosphere to the PPEF, have been described previously [e.g., *Zhao et al*., 2012, and references therein], and we will thus not repeat them here.

[10] Figure 2a plots an overview of observations during the superstorm. It begins at 0804 UT as seen from the SYMH index, which is essentially a 1 min resolution version of the Dst. The magnitude of the electric field in the polar region starts to increase as can be inferred from the CPCP enhancement. The three pairs of stations in Peru, India, and Japan always cover both daytime and nighttime at any moment. As response to the first pulse of solar wind dynamic pressure, the ΔH in India at 1304 LT increases by 80.1 nT, but the ΔH in Peru at 0304 LT and the ΔH in Japan at 1646 LT have changes less than 10 nT. Note that India and Japan have only a 3.7 h difference in local time. This suggests that there exist both longitude dependence and local time dependence in the response of ΔH to the PPEF. The CPCP is saturated during the late main phase and early recovery phase of the storm (1131–1944 UT), and the variations of the CPCP are consistent with those of the solar wind dynamic pressure rather than the IMF; more importantly, the PPEF is consistent with the CPCP [*Wei et al*., 2012].

[11] Figure 2b plots a closer view of the CPCP and ΔH to examine the PPEF effects. Taking CPCP as an indicator of the source of the PPEF, the PPEF signature becomes

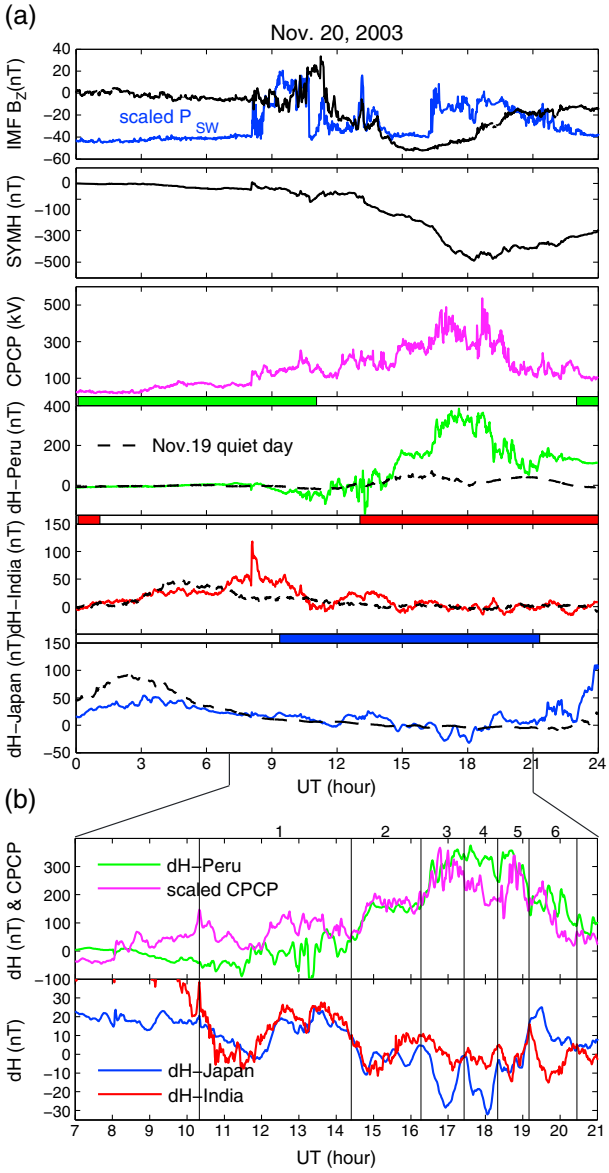

Figure 2. (a) In the first panel, the black line is IMF B_Z and the blue line is the scaled solar wind dynamic pressure (P_{SW}*3–50 in nPa). The SYMH index is shown in the second panel and the CPCP calculated by AMIE procedure in the third panel. The ΔH values inferred from the observations obtained using two geomagnetometers in Peru, India, and Japan are shown in the fourth, fifth, and sixth panels, respectively. The dashed line gives the quiet level measured on 19 November as a reference. The color/white bar illustrates the local nightside/dayside interval. (b) Comparisons of ΔH in Peru and CPCP (first panel) as well as ΔH values in Japan and India (second panel). The six intervals labeled by numbers are discussed in the text. The seven lines correspond to (from left) 1020, 1424, 1616, 1726, 1820, 1910, and 2027 UT.

discernible at all three longitudes after 1020 UT (the left vertical line). Around 1020 UT, a southward IMF pulse causes an enhancement of the CPCP, and the ΔH in India at 1520 LT (day) and the ΔH in Japan at 1902 LT (night) show a corresponding pulse. The IMF remains northward during 1024–1124 UT and results in a reduction of the CPCP. As a response, the ΔH levels in India and Japan decrease. Taking an overview of interval 1 (1020–1424 UT), the ΔH in Peru is not correlated with the CPCP, but the ΔH levels in India and Japan are. This is a local time dependence of the direction of the PPEF. As suggested by *Nopper and Carovillano* [1978], a duskward IEF may cause an eastward PPEF in the midnight-dawn sector and a westward PPEF in the other local time sector. Furthermore, the point in local time at which the PPEF changes direction changes day by day [*Wei et al.*, 2008a]. Note that an eastward PPEF corresponds to a positive ΔH. For this superstorm, we find that the PPEF changes direction around 1424 UT for all three longitudes, although it is not known why there is such a coincidence. We label four CPCP positive pulses with intervals 2–5. During each interval, the ΔH in Peru at daytime is correlated with the CPCP, but the ΔH levels in Japan and India at nighttime are not. Furthermore, the significant discrepancy between the Japan ΔH and the India ΔH also suggests a longitude dependence of the PPEF. As seen from the positive correlation between the Japan ΔH and the CPCP, the PPEF changes direction again around 1910 UT in Japan but does not change in Peru and India. In addition, Figure 2b shows that the magnitude of ΔH in Peru at daytime is greater than that at nighttime by about 1 order; it also shows that the magnitude of ΔH in Japan at nighttime is greater than that in India.

[12] What has become clear is that the night ΔH indeed can manifest a PPEF, but probably with significant variability caused by other factors, at least including local time dependence and longitude dependence of the PPEF itself. To study these two factors, we now turn to the multiple-penetration event.

2.3. Extraction of the PPEF With Band-Pass Filtering

[13] We first extract PPEF signals from all data sets. Figure 3 shows the 6 days (11–16 November 2003) of original data in black for the CPCP (first panel) and ΔH (third to fifth panels) as well as in cyan for the electric field (E-ISR) derived from vertical drift (second panel) through E (mV/m) = V (km/s)/40. The time resolution is 5 min for the ISR vertical drift, while it is 1 min for the others. Due to the neutral wind dynamo, the vertical drift and ΔH include a very strong diurnal effect. Figure 4 shows the power spectrum of the CPCP, vertical drift, and JIC-PIU ΔH using fast Fourier transform; one can see that the power of the 24 h period variation is overwhelming in all data sets. We thus use a band-pass filter to extract PPEF signals. The upper limit is set to 8 h, considering that the magnetosphere acts as a band-pass filter with a high pass near 8 h as suggested by *Kelley and Dao* [2009], while the lower limit is set to 0.25 h. The filtered data are also shown in Figure 3 with a different color from the original data. Note that the time resolution of all filtered data is 5 min for the following comparison with the vertical drift data. Since previous studies [*Wei et al.*, 2008a; *Kelley and Dao*, 2009] have already revealed that most of the fluctuations in ISR data originated from penetration of the IEF, here we treat the filtered ISR data as a "standard" PPEF. To evaluate the performance of ΔH in response to the PPEF on both the dayside and the nightside, the correlation coefficients between filtered ISR data and filtered ΔH will be discussed in the next section.

[14] However, there are still two caveats: (1) In the vertical drift (second panel in Figure 3), the pre-reversal enhancement

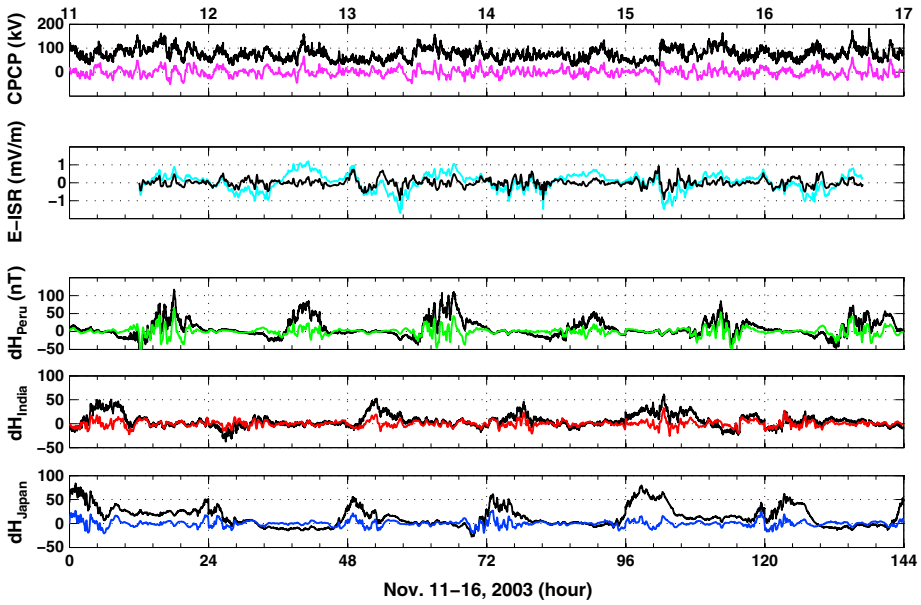

Figure 3. Original data and band-pass-filtered data during 11–16 November 2003. From top to bottom: CPCP derived by AMIE procedure, vertical drift measured by the JIC ISR (E-ISR), JIC-PIU ΔH, TIR-ABG ΔH, and YAP-BIK ΔH. The original data are shown in black for CPCP and ΔH values. For ISR vertical drift (second panel), the black color is used for filtered data. The color style for the filtered data applies to the other figures.

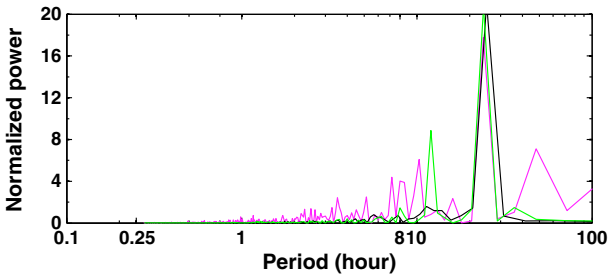

Figure 4. Normalized power spectrum (divided by its standard deviation) of unfiltered CPCP (magenta), E-ISR (black), and JIC-PIU ΔH (green).

is still discernible, especially around 49 UT and 120 UT (LT = UT − 5), and this decreases the calculated correlation coefficients between the CPCP and the PPEF. (2) Fluctuations with periods less than 15 min exist in all data sets but were not included in the present work due to the requirement of the band-pass filtering. This kind of short-term electric field pulses is expected to penetrate the equatorial ionosphere without significant shielding, because the ring current usually takes time to adjust to shield the newly formed PPEF [*Wolf et al.*, 2007].

2.4. Evaluation of the Global Coherence of the PPEF

[15] Since the penetration efficiency of the PPEF has strong local time dependence [*Nopper and Carovillano*, 1978], we have calculated correlation coefficients within a 2 h width sliding window and moved this window by 1 h for each step. Figure 5 shows the calculated correlation coefficients between scaled E-ISR and CPCP (Figure 5a), JIC-PIU ΔH (Figure 5b), TIR-ABG ΔH (Figure 5c), and YAP-BIK ΔH (Figure 5d). The upper panel of each part shows the filtered data, while the lower panel shows the correlation coefficients. In the middle, the white and colored blocks represent local daytime and nighttime, respectively. For example, the black line is filtered E-ISR and the white and black blocks represent the local daytime and nighttime in Peru, respectively. The color style of curves and the nighttime indicator have the same meaning as described for Figure 3. The results for YAP-OKI ΔH are given in brown (Figure 5d) for comparison, and they are discussed in the following.

[16] With a 2-D ionospheric electric field model, *Nopper and Carovillano* [1978] simulated the combined effect of the PPEF and the shielding electric field at the equator. They showed that a duskward IEF can cause a westward PPEF at the midnight-dawn sector and an eastward PPEF at the other local time sector. In fact, the global distribution of the PPEF is largely affected by that of conductivity, which is significantly modified by particle and energy precipitation on the auroral oval. As a result, the direction of the PPEF at the equator is found to vary from day to day [*Wei et al.*, 2008a]. Figure 5a also reveals such a variable pattern: the correlation coefficients between the PPEF and the CPCP are mostly positive on the dayside, but the negative coefficients are highly variable on the nightside. Since this work aims to study the performance of ΔH in response to the PPEF, we cannot initially hypothesize that all variations in the CPCP must cause the PPEF at the equator. Instead, it is reasonable to assume that all PPEF pulses are of global scale and that their magnitudes have local time dependence. Thus, we will use E-ISR as a "standard" PPEF and then compare all ΔH levels with E-ISR in Figures 5b–5d.

[17] Figure 5b shows E-ISR and JIC-PIU ΔH and their correlation. Note that the two data sets are recorded in the same place. For the most part of the daytime (0700–1600 LT), they

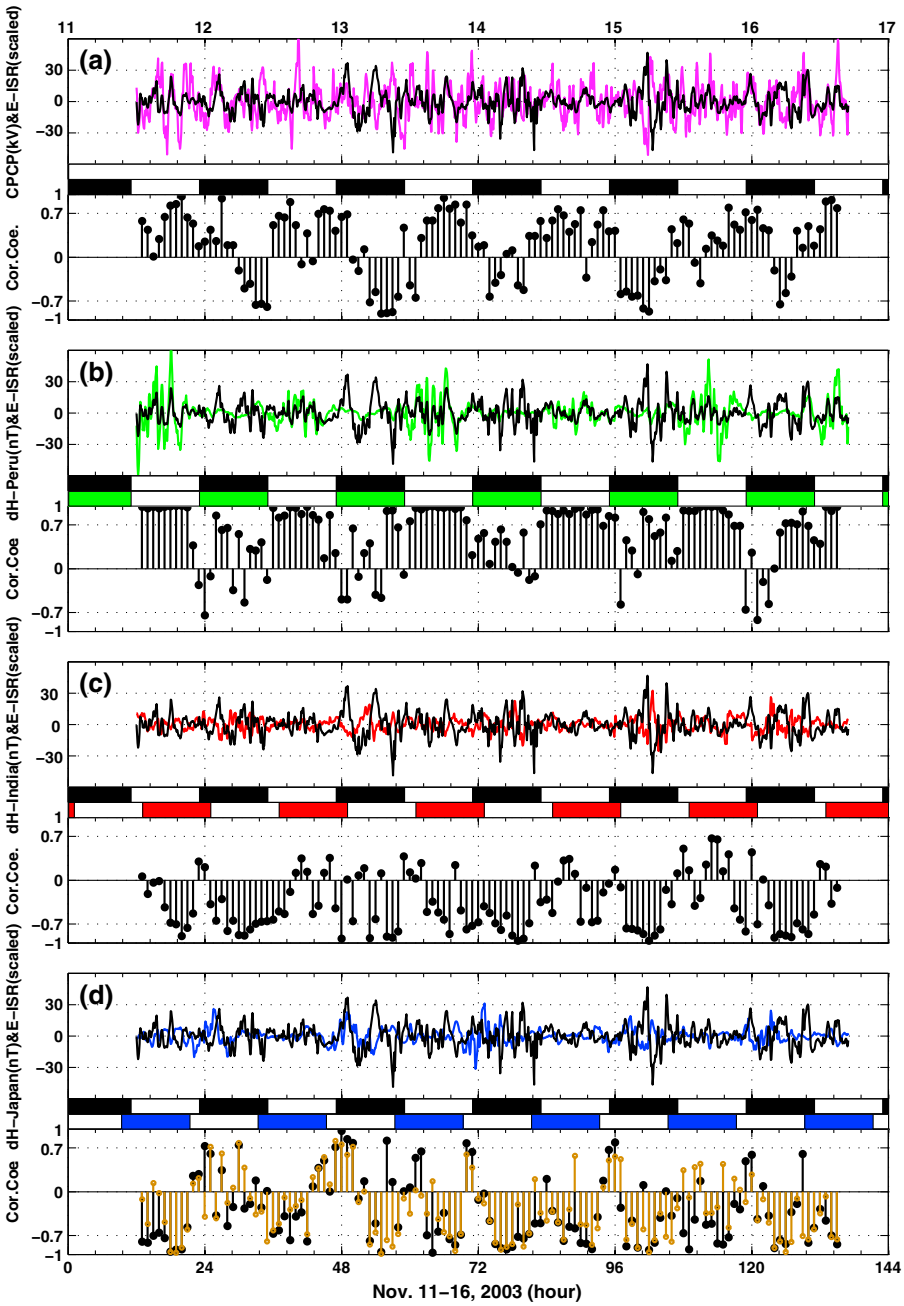

Figure 5. Correlation coefficients between the filtered data using a sliding window (see the text). (a) CPCP (magenta) and E-ISR (black). (b) E-ISR (black) and JIC-PIU ΔH (green). (c) E-ISR (black) and TIR-ABG ΔH (red). (d) E-ISR (black) and YAP-BIK ΔH (blue). For each part, the top panel plots the filtered data, the middle white/color bars illustrate local time with the color of nighttime corresponding to that in the upper panel, and the bottom panel shows the correlation coefficients. Note that the E-ISR is scaled for comparison with other data. In Figure 5d, the correlation coefficients (brown) between E-ISR and YAP-OKI ΔH are also shown for comparison.

have a very strong correlation, as already concluded by *Anderson et al*. [2002]. Around the dusk terminator (1600–2000 LT), the correlation coefficients are highly variable. The first reason for this is that the PPEF usually weakens and then changes its direction from eastward to westward, and the second reason is that the pre-reversal enhancement is not related to the PPEF, as mentioned in the caveats in section 2.3. Due to the uncertainties, these coefficients have less meaning for our purpose. Note that the first reason can also explain the low coefficients around the morning terminator (0500–0700 LT). For the rest of the nighttime (2000–0500 LT), the coefficients are mostly positive, but they still significantly change day by day. A striking finding is that the coefficients remain around 0.7 in the midnight-dawn sector (0000–0500 LT) on 15 and 16 November. Therefore, at least for these 2 days, the

nightside ΔH correlates with the PPEF in the midnight-dawn sector. *Fejer et al*. [2007] also found that the ΔH at 0400–0600 LT showed exceptionally large PPEF signatures. Considering that we have examined data from 6 days, 2 of 6 suggests a 33% chance to observe a nightside ΔH correlation with the PPEF in Peru.

[18] Figure 5c shows E-ISR and TIR-ABG ΔH and their correlation. There is a 14 h lag in local time between Peru and India. Taking an overview, the coefficients are mostly negative; i.e., E-ISR and TIR-ABG ΔH are roughly anti-correlated. For 2 days (11 and 13 November) during 11–15 November, the coefficients remain around 0.7 in the midnight-dawn sector. This suggests a 40% chance to observe a nightside ΔH correlation with the PPEF in India, if we suppose that the PPEF always has a global coherence.

[19] Figure 5d shows E-ISR and YAP-BIK ΔH in the upper panel as well as the correlation coefficients between E-ISR and YAP-BIK ΔH (black) and between E-ISR and YAP-OKI ΔH (brown). There is also a 14 h difference in local time between Peru and Japan. Taking an overview, the coefficients are also mostly negative, but with more positive values compared to Figure 5c. The performance of YAP-BIK ΔH and that of YAP-OKI ΔH (brown) roughly agree but occasionally show a large discrepancy (e.g., 13 November). For 3 days (11, 13, and 14 November) during 11–15 November, the coefficients remain around 0.7 in the midnight-dawn sector. This suggests a 60% chance to observe a nightside ΔH correlation with the PPEF in Japan.

[20] The nightside ΔH in the midnight-dawn sector indeed can indicate the PPEF, but not always. Within 6 days and at three longitudes, the observations suggested that one has a 33%–60% chance to observe this phenomenon on a given day. We should emphasize that these percentages were derived from very limited data sets and that the time interval of samples was 1 day. This chance of about 50%, if eventually proven to be consistent with the results derived from a larger database in the future, implies that there is no clear tendency for a nightside ΔH correlation with the PPEF or at least not during the moderate geomagnetic disturbance time ($Dst > -60$ nT).

[21] Now we examine these coefficients in more detail. Since the coefficients exhibit significant dependence on local time, we plot them against local time in Figure 6. In Peru, the E-ISR and ΔH have correlation coefficients above 0.7 during 0700–1600 LT, but there is no clear trend for the nighttime. One discernible finding is that the coefficients in the midnight-dawn sector are more concentrated above the zero line than those in the dusk-midnight sector. In India, the distribution pattern is quite similar to that in Peru but with a reversed sign, suggesting the global coherence of the PPEF. In Japan, both YAP-BIK ΔH and YAP-OKI ΔH have a very scattered distribution. It is difficult to understand why the ΔH has such a significant longitude bias in Asia, considering the longitude difference is only 56°. Nevertheless, YAP-BIK ΔH in the midnight-dawn sector exhibits a better correlation with E-ISR compared to YAP-OKI ΔH. The "0.6" label on the YAP-BIK panel means 60% of the coefficients are at or above 0.7 in the midnight-dawn sector.

[22] An alternative way to evaluate the overall correlation, instead of a sliding window, is a scatterplot of all 6 days of data. Figure 7 plots E-ISR versus ΔH during the daytime (0700–1700 LT) in blue and the midnight-dawn (0000–0500 LT) in black. On each subplot, the label "r" is the correlation coefficient and "a" and "b" are the coefficients for linear fitting [ΔH (nT) = a*E-ISR (mV/m) + b]. For the dayside ΔH, the r is the largest (0.9) in Peru, without surprise. However, it is 0.6 in India while only 0.1–0.2 in Japan. This shows a significant longitude bias of ΔH as an indicator of the PPEF although the PPEF is of global scale; i.e., the dayside ΔH in India has a better correlation with the nightside vertical drift than the dayside ΔH in Japan. The low value of r in Japan contradicts the opinion that the PPEF is of global scale as shown by simulations [e.g., *Nopper and Carovillano*, 1978] and observations [e.g., *Kelley et al*., 2007]. Considering the highly scattered pattern of correlation coefficients shown in Figure 6, this low value of r in Figure 7

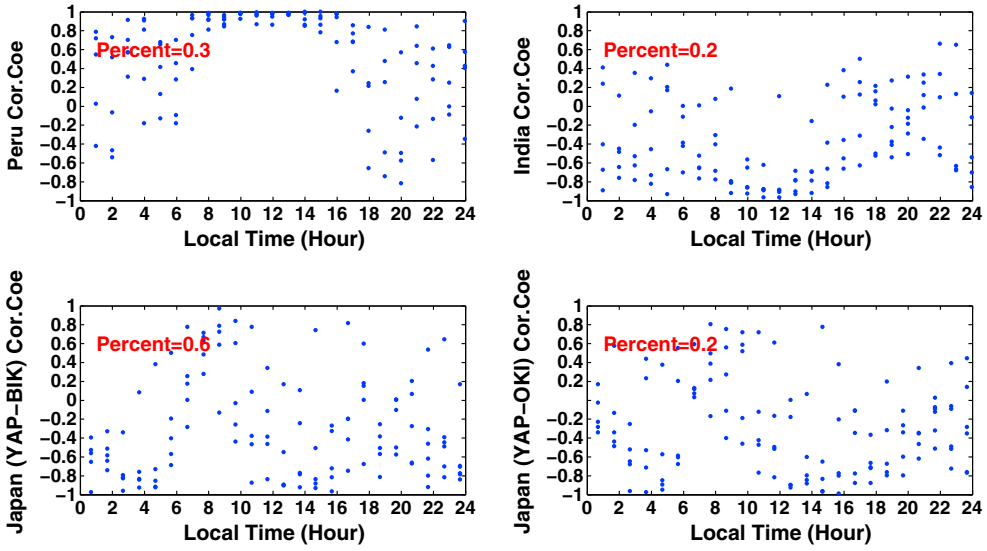

Figure 6. Local time distribution of the correlation coefficients shown in Figure 5. "Percent" represents the percentage of coefficients that are equal to or higher than 0.7 at 0000–0500 LT.

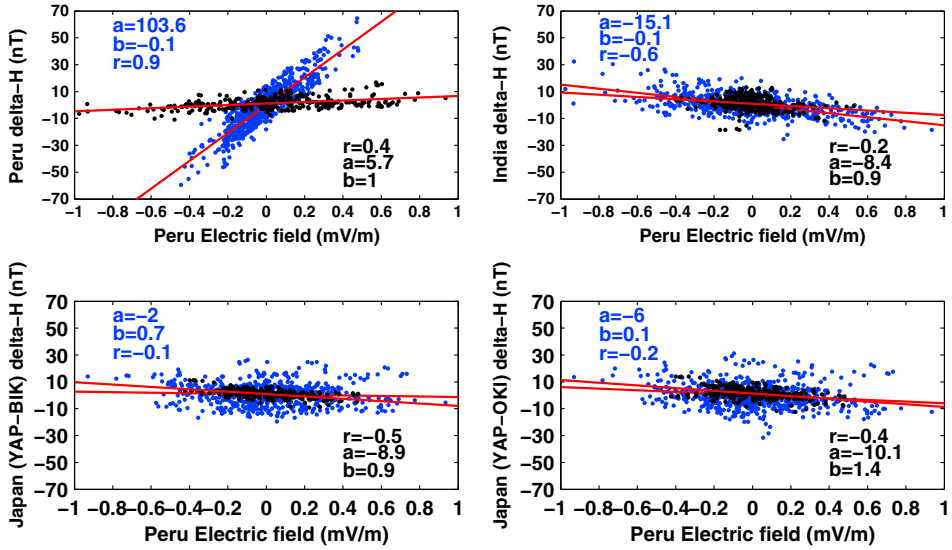

Figure 7. Scatterplots of E-ISR and ΔH values during the daytime (0700–1700 LT) in blue and from midnight to dawn (0000–0500 UT) in black. On each subplot, "r" is the correlation coefficient and "a" and "b" are the coefficients for linear fitting (ΔH = a*E-ISR + b).

indeed reflects the weak correlation between the dayside PPEF in Japan and the nightside PPEF in Peru. Nevertheless, during the midnight-dawn interval, the r is −0.5 for YAP-BIK ΔH, with an absolute value even greater than that in Peru (0.4). This suggests that the longitude bias of ΔH as an indicator of the PPEF also exists on the nightside; i.e., the ΔH in the midnight-dawn sector in Japan has a better correlation with the dayside vertical drift.

[23] In Peru, the data show two different linear relations for these two intervals. Comparing "a" on the dayside with that on the nightside, we find that the magnitude of the nightside ΔH in the sector is about 1/18 (5.7/103.6) of that of the dayside ΔH as a response to a given PPEF. But the ratios calculated for India and Japan are meaningless, because the values of r are quite low.

2.5. Latitude Profile of the H Component

[24] The results presented above show that the nightside ΔH can manifest a PPEF, at least occasionally. To understand this phenomenon further, one needs to know the meaning of nightside ΔH. Here we take the observations during 11 November 2003 as an example to investigate its meaning. There are a large PPEF pulse on the dayside and a large PPEF pulse on the nightside as well. Figure 8 plots the original data (without filtering). The top panel shows that JIC-PIU ΔH agrees with E-ISR (black) very well on the dayside. In the middle panel, it is discernible that there is a correlation between the nightside TIR-ABG ΔH and E-ISR during 1500–2400 UT (2000–0500 LT). However, the magnitude of these variations in the nightside TIR-ABG ΔH was very small. In the bottom panel, YAP-BIK ΔH (blue) and YAP-OKI ΔH (brown) exhibit significant discrepancy on the whole, but the short-term fluctuations, i.e., PPEF, were roughly consistent with each other, and both showed a discernible correlation with E-ISR. The CPCP (magenta) is also plotted here to show the origin of the PPEF. We will focus on one increase on the dayside and one decrease on the nightside, as illustrated by the vertical lines, and both were associated with an enhancement of the CPCP.

[25] Figure 9 shows the latitude profile of the H component from the northern mid-latitude to the southern mid-latitude in the Japan sector. On the dayside, the H component at YAP is the strongest among those at the low-latitude stations, indicating the existence of an EEJ. The PPEF signatures are

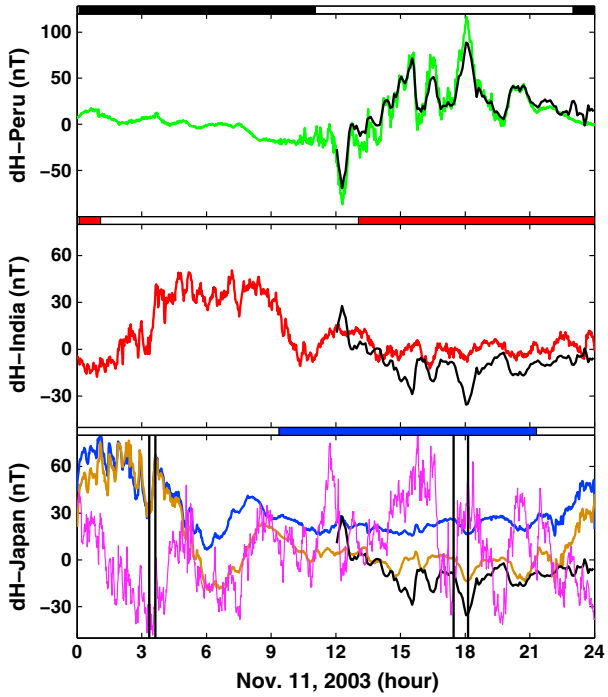

Figure 8. Unfiltered CPCP, E-ISR, and ΔH values during 11 November 2003. The color style is the same as that in Figure 3. The vertical lines mark dayside and nightside PPEF enhancements.

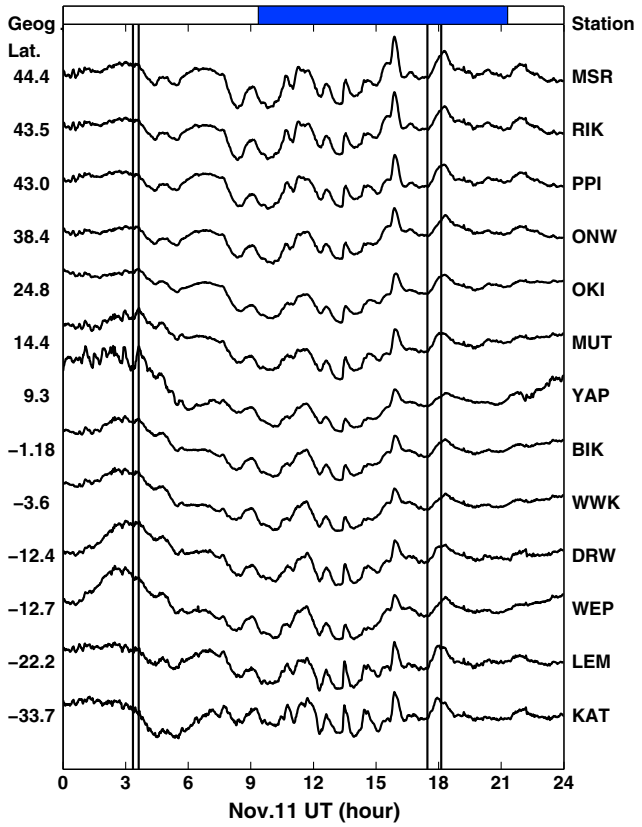

Figure 9. The geomagnetic H component observed by the mm210 station chain for which the locations are shown in Figure 1 and Table 1. Their geographic latitudes are marked on the left side. To avoid overlapping, the H components have been offset by 100 nT for one station to the neighbor. The vertical line is the same as that in Figure 8.

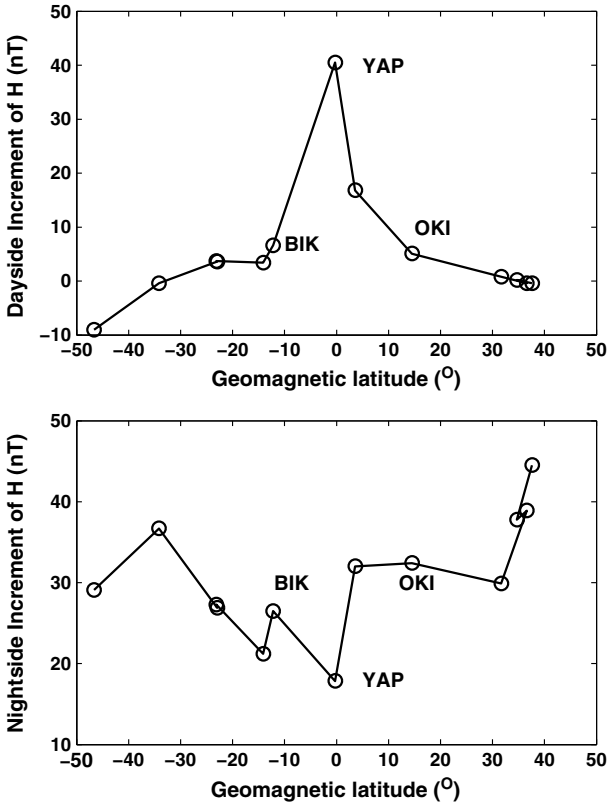

Figure 10. Latitude profiles of the increments in H components during the two intervals marked by vertical lines in Figures 8 and 9.

only notable at YAP and MUT. This forces us to give a warning here: one should be cautious when calculating ΔH with two off-equator stations (without a station strictly at the geomagnetic equator) for some weak or moderate storms, although it has been found to work for some intense storms or superstorms. For example, *Galav et al*. [2011] used HAT (geomagnetic latitude 23.9°N) and GUA (geomagnetic latitude 5.0°N), while *Li et al*. [2009] used MUT (geomagnetic latitude 3.6°N) and PHU (geomagnetic latitude 7.1°N) to discern PPEF signatures and acquired reasonable results. But we do not recommend regularly using this method. Figure 9 shows that if we use MUT as an "on-equator station" to calculate ΔH, the inferred PPEF will be significantly underestimated compared to the case using YAP. On the nightside, the variations in the H component at YAP are the weakest among all stations, and this is opposite to the situation on the dayside.

[26] Now let us turn to the PPEF signatures during the two intervals of interest (marked by vertical lines). Figure 10 plots the increment of the H component (subtracting the value at the first vertical line from the value at the second vertical line) at each station during each interval. On the dayside, it is clear that the EEJ effect dominates near the equator, as described by *Anderson et al*. [2002]. For this interval, YAP-BIK and YAP-OKI give a similar ΔH. On the nightside, the increment of the H component at YAP is smallest, and the ΔH is negative. This can explain why the correlation coefficients between JIC-PIU ΔH and E-ISR were mostly positive during the nightside and thus also supports that "nightside ΔH can manifest a PPEF." The dayside ΔH is produced with the H at an on-equator station being greater than the H at an off-equator station, while the nightside ΔH, on the contrary, is produced with the H at an on-equator station being smaller than the H at an off-equator station. The latitude profiles also suggest that the source current for the dayside ΔH is located at the equator, while the source current for the nightside ΔH is located at a high-latitude region. In other words, the nightside ΔH was caused by attenuation of the effects of the polar electric field with decreasing latitude. In addition, here one can see YAP-BIK and YAP-OKI gave different nightside ΔH values; thus, the distance between the two ΔH stations can also affect evaluation of the correlation between the PPEF and the nightside ΔH.

3. Discussion

[27] We have analyzed the relationship between the PPEF measured by ISR in Peru and ΔH in Peru, India, and Japan during a superstorm and a multiple-penetration event. The multiple-penetration event provides a unique database that allows us to examine the performance of the nightside ΔH in response to the PPEF. The band-pass-filtered data still contained electric field components without a fixed period or unrelated to the PPEF, for example, a pre-reversal enhancement and disturbance dynamo. The former appears

around the dusk, while the latter could be stronger on the whole nightside. Thus, both of them might introduce uncertainty in the correlation between PPEF and nightside ΔH as shown in the data. However, since our event consists of many PPEF pulses, the results presented in this paper could provide some clues with statistical meaning.

[28] If treating the ionosphere as a 2-D shell, geomagnetic variations can be regarded as the effects of the equivalent current systems on the ionosphere. The ΔH itself is directly related to the gradient of the equivalent current system over these stations. On the dayside equator, the EEJ flows in a narrow band along the equator and thus produces a strong gradient around the boundary of the band, pointing toward the equator. On the nightside, as shown in Figure 10, the gradient points toward the polar region and the value of gradient is much smaller than that of the highly localized EEJ. Therefore, the correlation between electric field and ΔH must be less significant compared to that on the dayside.

[29] Through examining the filtered data by a sliding window method, we found that a good correlation (0.7) appears in the midnight-dawn sector. The local time bias can be understood by previous simulations [e.g., *Nopper and Carovillano*, 1978; *Wei et al*., 2008c], which showed that the PPEF is the strongest in the midnight-dawn sector. A puzzling finding is that the ΔH in the midnight-dawn sector in Japan has a higher correlation coefficient with the PPEF in Peru compared with the ΔH in Peru itself (Figure 7). *Fejer et al*. [2007] and *Galav et al*. [2011] also reported that the nightside ΔH in Japan can react to the PPEF. More data need to be examined to understand this longitude bias.

[30] With the physical picture simulated by *Nopper and Carovillano* [1978], we may explain how the nightside ΔH responds to the PPEF. The polar cap electric field propagates to the equator with attenuation; since there is no significant Cowling conductivity on the nightside equatorial ionosphere, the current associated with the PPEF also attenuates with decreasing latitude; and the gradient of the PPEF-driven current contributes to the nightside ΔH. Given the gradient is a constant, the greater the PPEF is, the greater the ΔH is. Since the PPEF has its maximum of magnitude in the midnight-dawn sector, the ΔH should have more chance to show its response to the PPEF in this sector.

[31] Based on the results presented in this paper, we suggest that one may identify a PPEF by comparing ΔH in the 0000–1800 LT sector with the electric field in the upstream solar wind or the polar ionosphere. The general suggestions for usage of ΔH are as follows. For the dayside case, JIC-PIU ΔH and TIR-ABG ΔH are suitable for investigating the global coherence of the PPEF, as shown in Figure 6. Although Japan also has a 10 h difference in local time with Peru, the overall correlation between them is relatively weak compared to that between India and Peru. Comparing the performance of YAP-OKI ΔH and YAP-BIK ΔH (Figures 6 and 9), there is no significant difference for the daytime interval. From Figure 9, as mentioned in section 2.5, it is better to include a station strictly on the geomagnetic equator. The ΔH by two off-equator stations probably significantly underestimates or even misses the PPEF. For the nightside case, the ΔH in the midnight-dawn sector may be used if it indeed shows good correlation with the IEF or polar cap electric field. As shown in Figures 6 and 7, YAP-BIK ΔH is the best candidate in our database. But we should emphasize that the Dst is greater than −60 nT during the multiple-penetration event. The conclusions derived from this multiple-penetration event are perhaps not suitable for intense storms and superstorms, during which magnetosphere-ionosphere coupling is much more complicated.

4. Conclusions

[32] The data set derived from the multiple-penetration event suggests that the nightside ΔH can manifest a PPEF in the midnight-dawn sector (0000–0500 LT), but not always. One has a 33%–60% chance to observe this phenomenon for a given day. The magnitude of ΔH on the nightside sector was only 1/18 of that of ΔH on the dayside in response to the same PPEF. The latitude profile of the H component recorded by the mm210 station chain suggests that PPEF-driven nightside ΔH is produced by the attenuation of PPEF-driven current from high latitude to the equator.

[33] The data set derived from the multiple-penetration event also suggests a longitude bias of the response of ΔH to the PPEF. The ΔH on the dayside in India has a better correlation with the vertical drift on the nightside in Peru, while the ΔH in the midnight-dawn sector in Japan has a better correlation with the vertical drift on the dayside in Peru. We suggest that one may identify a PPEF by comparing ΔH in the 0000–1800 LT sector through comparing with the electric field in the upstream solar wind or the polar ionosphere. But please note that these conclusions are deduced from a case with $Dst > -60$ nT. More assessments need to be conducted before using nightside ΔH as a regular parameter to identify electric field penetration.

[34] **Acknowledgments.** This work was supported by grant WO910/3-1 within the priority program "Planetary Magnetism" of the Deutsche Forschungsgemeinschaft (DFG) and grant 50QM0801 of the German Aerospace Agency (DLR). The work in China was supported by the National Science Foundation of China (41004072 and 41174138) and the National Important Basic Research Project (2011CB811405). The Jicamarca Radio Observatory is a facility of the Instituto Geofísico del Perú operated with support from the NSF Cooperative Agreement ATM-0432565 through Cornell University. NCAR is supported by the U.S. National Science Foundation. We sincerely thank Dr. R. Pandey for giving valuable suggestions and Dr. Ridley for providing the AMIE-derived CPCP data.

References

Anderson, D., A. Anghel, K. Yumoto, M. Ishitsuka, and E. Kudeki (2002), Estimating daytime vertical ExB drift velocities in the equatorial F-region using ground-based magnetometer observations, *Geophys. Res. Lett.*, *29*(12), 1596, doi:10.1029/2001GL014562.

Bell, J., M. Gussenhoven, and E. Mullen (1997), Super storms, *J. Geophys. Res.*, *102*(A7), 14189–14198.

Blanc, M., and A. D. Richmond (1980), The ionospheric disturbance dynamo, *J. Geophys. Res.*, *85*, 1669.

Fejer, B. G., J. W. Jensen, T. Kikuchi, M. A. Abdu, and J. L. Chau (2007), Equatorial Ionospheric Electric Fields During the November 2004 Magnetic Storm, *J. Geophys. Res.*, *112*, A10304, doi:10.1029/2007JA012376.

Fejer, B. G. (2002), Low latitude storm time ionospheric electrodynamics, *J. Atmos. Sol.-Terr. Phys.*, *64*, 1401.

Fejer, B. G., and L. Scherliess (1997), Empirical models of storm-time equatorial zonal electric fields, *J. Geophys. Res.*, *102*, 24,047–24,036.

Galav, P., S. Sharma, and R. Pandey (2011), Study of simultaneous penetration of electric fields and variation of total electron content in the day and night sectors during the geomagnetic storm of 23 May 2002, *J. Geophys. Res.*, *116*, A12324, doi:10.1029/2011JA017002.

Huang, C.-S., K. Yumoto, S. Abe, and G. Sofko (2008), Low-latitude ionospheric electric and magnetic field disturbances in response to solar wind pressure enhancements, *J. Geophys. Res.*, *113*, A08314, doi:10.1029/2007JA012940.

Huang, C.-S., J. C. Foster, and M. C. Kelley (2005), Long-duration penetration of the interplanetary electric field to the low-latitude ionosphere during the main phase of magnetic storms, *J. Geophys. Res.*, *110*, A11309, doi:10.1029/2005JA011202.

Kelley, M. C., and E. Dao (2009), On the local time dependence of the penetration of solar wind-induced electric fields to the magnetic equator, *Ann. Geophys.*, *27*, 3027–3030.

Kelley, M. C., M. J. Nicolls, D. Anderson, A. Anghel, J. L. Chau, R. Sekar, K. S. V. Subbarao, and A. Bhattacharyya (2007), Multi-longitude case studies comparing the interplanetary and equatorial ionospheric electric fields using an empirical model, *J. Atmos. Sol.-Terr. Phys.*, *69*(10–11), 1174–1181.

Kelley, M. C., J. J. Makela, J. L. Chau, and M. J. Nicolls (2003), Penetration of the solar wind electric field into the magnetosphere/ionosphere system, *Geophys. Res. Lett.*, *30*(4), 1158, doi:10.1029/2002GL016321.

Kelley, M. C. (1989), The Earth's Ionosphere Plasma Physics and Electrodynamics, Academic, San Diego, CA.

Kikuchi, T., Y. Ebihara, K. K. Hashimoto, R. Kataoka, T. Hori, S. Watari, and N. Nishitani (2010), Penetration of the convection and overshielding electric fields to the equatorial ionosphere during a quasiperiodic *DP* 2 geomagnetic fluctuation event, *J. Geophys. Res.*, *115*, A05209, doi:10.1029/2008JA013948.

Kikuchi, T., H. Luehr, T. Kitamura, O. Saka, and K. Schlegel (1996), Direct penetration of the polar electric field to the equator during a DP 2 event as detected by the auroral and equatorial magnetometer chains and the EISCAT radar, *J. Geophys. Res.*, *101*, 17,161–17,173, doi:10.1029/96JA01299.

Li, G., B. Ning, B. Zhao, L. Liu, W. Wan, F. Ding, J. S. Xu, J. Y. Liu, and K. Yumoto (2009), Characterizing the 10 November 2004 storm-time middle-latitude plasma bubble event in Southeast Asia using multi-instrument observations, *J. Geophys. Res.*, *114*, A07304, doi:10.1029/2009JA014057.

Nishida, A. (1968), Coherence of geomagnetic DP 2 fluctuations with interplanetary magnetic variations, *J. Geophys. Res.*, *73*(17), 5549.

Nopper, R. W., Jr., and R. L. Carovillano (1978), Polar-equatorial coupling during magnetically active periods, *Geophys. Res. Lett.*, *5*(8), 699–702.

Rastogi, R. G., Geomagnetic storms and electric fields in the equatorial ionosphere, *Nature*, *268*, 422, 1977.

Richmond, A. D., and Y. Kamide (1988), Mapping electrodynamic features of the high-latitude ionosphere from localized observations: Technique, *J. Geophys. Res.*, *93*, 5741–5759.

Ridley, A. J., G. Lu, C. R. Clauer, and V. O. Papitashvili (1998), A statistical study of the ionospheric convection response to changing interplanetary magnetic field conditions using the assimilative mapping of ionospheric electrodynamics technique, *J. Geophys. Res.*, *103*, 4023–4039.

Tsurutani, B. T., E. Echer, F. L. Guarnieri, and W. D. Gonzalez (2010), The properties of two solar wind high speed streams and related geomagnetic activity during the declining phase of solar cycle 23. *J. Atmos. Sol. Terr. Phys.*, *73*, 164–177, doi:10.1016/j.jastp.2010.04.003.

Veenadhari, B., S. Alex, T. Kikuchi, A. Shinbori, R. Singh, and E. Chandrasekhar (2010), Penetration of magnetospheric electric fields to the equator and their effects on the low-latitude ionosphere during intense geomagnetic storms, *J. Geophys. Res.*, *115*, A03305, doi:10.1029/2009JA014562.

Wei, Y., W. Wan, B. Zhao, M. Hong, A. Ridley, Z. Ren, M. Fraenz, E. Dubinin, and M. He (2012), Solar wind density controlling penetration electric field at the equatorial ionosphere during a saturation of cross polar cap potential, *J. Geophys. Res.*, *117*, A09308, doi:10.1029/2012JA017597.

Wei, Y., W. Wan, Z. Pu, M. Hong, Q. Zong, J. Guo, B. Zhao, and Z. Ren (2011), The transition to overshielding after sharp and gradual interplanetary magnetic field northward turning, *J. Geophys. Res.*, *116*, A01211, doi:10.1029/2010JA015985.

Wei, Y., et al. (2010), Long-lasting goodshielding at the equatorial ionosphere, *J. Geophys. Res.*, *115*, A12256, doi:10.1029/2010JA015786.

Wei, Y., et al. (2009), Westward ionospheric electric field perturbations on the dayside associated with substorm processes, *J. Geophys. Res.*, *114*, A12209, doi:10.1029/2009JA014445.

Wei, Y., et al. (2008a), Unusually long lasting multiple penetration of interplanetary electric field to equatorial ionosphere under oscillating IMF Bz, *Geophys. Res. Lett.*, *35*, L02102, doi:10.1029/2007GL032305.

Wei, Y., M. Hong, W. Wan, A. Du, Z. Pu, M. F. Thomsen, Z. Ren, and G. D. Reeves (2008b), Coordinated observations of magnetospheric reconfiguration during an overshielding event, *Geophys. Res. Lett.*, *35*, L15109, doi:10.1029/2008GL033972.

Wei, Y., M. H. Hong, W. X. Wan, and A. M. Du (2008c), A modeling study of interplanetary-equatorial electric field penetration efficiency, *Chin. J. Geophys.*, *51*, 1279–1284.

Wolf, R. A., R. W. Spiro, S. Sazykin and F. R. Toffoletto (2007), How the Earth's inner magnetosphere works: An evolving picture, *J. Atmos. Sol. Terr. Phys.*, *69*(3), 288–302, doi:10.1016/j.jastp.2006.07.026.

Zhao, B., et al. (2012): Positive ionospheric storm effects at Latin America longitude during the superstorm of 20–22 November 2003: revisit, *Ann. Geophys.*, *30*, 831–840, doi:10.5194/angeo-30-831-2012.